Chemistry–A European Journal
Research Article
doi.org/10.1002/chem.202400950
Chemistry Europe
European Chemical Societies Publishing
www.chemeurj.org

Afterglow Performance of Phenylenevinylene-Based Semiconducting Polymer Nanoparticles Doped with Photosensitizers Containing Electron-Withdrawing Groups

Ting-Jiao Shi,[a, b] Dong-Hui Wang,[d] Xu Zhao,[a, b] Li-Jian Chen,*[a, b] and Xiu-Ping Yan*[a, b, c]

It is usually believed that doping with photosensitizers capable of generating singlet oxygen ($^1O_2$) plays a pivotal role in enhancing the afterglow performance of semiconducting polymer nanoparticles (SPNs). However, the effect of doping photosensitizer bearing electron-withdrawing groups has not been reported. Here we report the effect of doping with six photosensitizers possessing different electron-withdrawing groups on the afterglow performance of SPNs using poly[(9,9-di(2-ethylhexyl)-9H-fluo-rene-2,7-vinylene)-co-(1-methoxy-4-(2-ethylhexyloxy)-2,5-phenylenevinylene)] (PF-MEHPPV) as substrate. It was found that the afterglow performance of SPNs was significantly influenced by doping with photosensitizers bearing electron-withdrawing groups. For the doped photosensitizers with strong electron-withdrawing groups, the stronger the electron-withdrawing ability of the group, the worse of the afterglow performance of the SPN regardless of the $^1O_2$ generation ability of the photosensitizer. When the doped photosensitizer exhibited weak or none electron-withdrawing effect, the $^1O_2$ generation ability of the photosensitizer played a dominant role on the afterglow performance of the SPNs. This work deepens the understanding of the design and synthesis of SPNs with different afterglow properties.

Introduction

Semiconducting polymer nanoparticles (SPNs), primarily made of π-conjugated polymers, have been demonstrated in a wide range of applications such as polymeric photovoltaics, biosensing, *in vivo* imaging and theranostics due to their excellent tunable optical and electronic properties.[1–6] The afterglow property of SPNs was reported for the first time in 2015.[7] The afterglow of this first example lasted nearly one hour after the cessation of white light excitation. The structural flexibility, unique optoelectronic property and no need for in situ excitation make SPNs promising for *in vivo* afterglow imaging and around-the-clock devices.[8–11] Unlike inorganic persistent luminescent nanoparticles, SPNs are completely organic without any heavy metal elements, avoiding the potential physiological toxicity for biomedical applications or environmental contamination for the manufacture of optoelectronic devices.[12–14]

To date, many kinds of SPNs have been reported for *in vivo* afterglow imaging applications. For example, a series of phenylenevinylene (PPV)-based SPNs were prepared from poly[2-methoxy-5-(2-ethylhexyloxy)-1,4-phenylenevinylene] (MEH-PPV) and its analogues.[15,16] It was found that only PPVs with electron-donating substituents (alkoxyl groups) exhibited detectable afterglow luminescence and SPN-MEHPPV showed the best afterglow performance. Other derivatives with weak electron-donating (alkyl groups) or strong electron-withdrawing substituents (cyano groups) did not show effective afterglow luminescence, indicating the effect of substituent groups. It was proposed that the afterglow of SPNs resulted from the photon generation from the degradation of the unstable PPV-dioxetane intermediate from the oxidation of the vinylene bond (C=C) of PPVs by singlet oxygen ($^1O_2$) under light excitation.[15] However, the afterglow luminescence of SPN-MEHPPV was still relatively low. In order to enhance the afterglow performance of SPNs, poly[(9,9-di(2-ethylhexyl)-9H-fluo-rene-2,7-vinylene)-co-(1-methoxy-4-(2-ethylhexyloxy)-2,5-phenylenevinylene)] (PF-MEHPPV) was used to replace MEH-PPV as an afterglow substrate.[17] Because the highest occupied molecular orbital of PF-MEHPPV was closed to the lowest unoccupied molecular orbital of dioxetane intermediates, the intermolecular electron transfer easily occurred to enhance the luminescence.

Doping photosensitizers is a popular strategy to increase the $^1O_2$ generation and enhance the afterglow emission.[18] For instant, doping tetraphenylporphyrin and silicon 2,3-naphthalocyanine bis(trihexylsilyloxide) (NCBS) into several SPNs significantly amplified the afterglow signal.[15,16,19–21] In addition, a

[a] T.-J. Shi, Dr. X. Zhao, Dr. L.-J. Chen, Prof. Dr. X.-P. Yan
State Key Laboratory of Food Science and Resources
Jiangnan University
Wuxi 214122, China
E-mail: chenlijian123@jiangnan.edu.cn
[b] T.-J. Shi, Dr. X. Zhao, Dr. L.-J. Chen, Prof. Dr. X.-P. Yan
Institute of Analytical Food Safety
School of Food Science and Technology
Jiangnan University
Wuxi 214122, China
[c] Prof. Dr. X.-P. Yan
Key Laboratory of Synthetic and Biological Colloids
Ministry of Education, School of Chemical and Material Engineering
Jiangnan University
Wuxi 214122, China
E-mail: xpyan@jiangnan.edu.cn
[d] Dr. D.-H. Wang
College of Food and Health
Zhejiang Agriculture and Forestry University
Hangzhou 311300, China.

Supporting information for this article is available on the WWW under https://doi.org/10.1002/chem.202400950

strategy was developed to power the afterglow emission by doping aggregation-induced emission (AIE) dyes as efficient $^1O_2$ generation reagents.[17] AIE dyes withstand aggregation-caused quenching effect, achieving effective $^1O_2$ generation and luminescence enhancement. It seems that increasing the generation of $^1O_2$ is an important approach to promote the afterglow performance of semiconducting polymers. However, it is not clear if doping with photosensitizers with electron-withdrawing substituents can still improve the afterglow performance of SPNs.

Herein, we report the effect of doping with photosensitizers possessing electron-withdrawing groups on the afterglow performance of SPNs. Six photosensitizers with different electron-withdrawing groups were doped into SPN-PF-MEHPPV to study the impact of their doping on the afterglow performance. Three of them are AIE molecules (WDH-001, WDH-006 and TPAM-2) possessing the same main body of triphenylamine but different substituents (cyano and carbonyl groups) with increasing electron-withdrawing ability. Another three are common photosensitizers (meso-tetra(4-carboxyphenyl) porphyrin (TCPP), chlorin e6 (Ce6), and NCBS) bearing the similar structure of porphine and with decreasing electron-withdrawing substituents (carboxyl groups). SPNs doped with these six photosensitizers were divided into two groups and subjected to either white LED or red LED illumination for investigation in view of their different absorption properties. The afterglow performance and the ability of $^1O_2$ generation of the SPNs doped with six photosensitizers were compared, and the impact of the electron-withdrawing ability and the $^1O_2$ generation ability of photosensitizers on the afterglow emission was discussed.

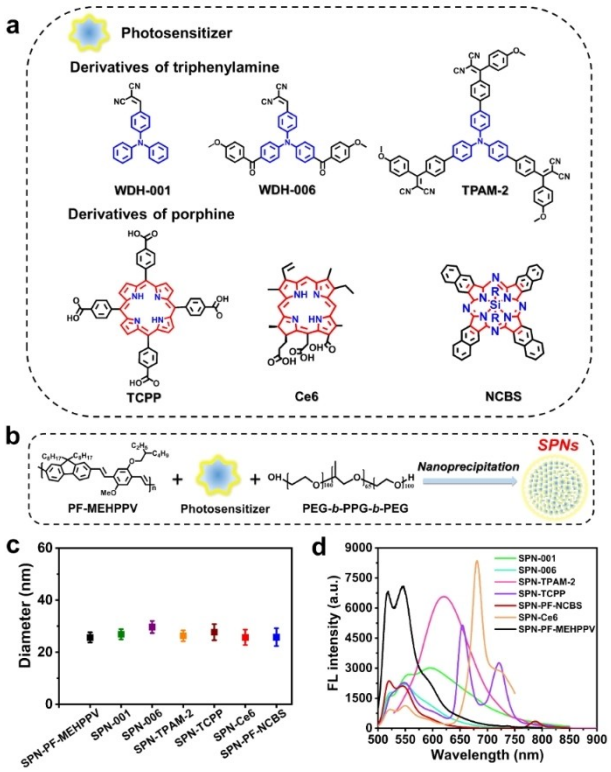

Figure 1. Design, preparation, and characterization of SPNs. (a) Chemical structures of the six photosensitizers doped in SPNs. (b) Schematic illustration for the preparation of SPNs. (c) Average hydrodynamic diameters of SPNs in aqueous solution. The error bars, ± one standard deviation (n = 3). (d) Fluorescence spectra of SPNs.

Results and Discussion

Design, Synthesis and Characterization of SPNs

Figure 1 shows the design, preparation and characterization of SPNs. Six photosensitizers with different electron-withdrawing groups including three AIE photosensitizers (WDH-001, WDH-006 and TPAM-2), and three common photosensitizers (TCPP, Ce6 and NCBS) (Figure 1a). TPAM-2 with strong fluorescence and high $^1O_2$ generation efficiency in the state of aggregation was reported in our previous report.[22] Two other molecules WDH-001 and WDH-006 were synthesized (Supporting information) and characterized by ^1H NMR and ESI-MS spectroscopy (Figure S1–S4). Both WDH-001 and WDH-006 showed the aggregation-induced fluorescence emission in the DMSO/water mixed solutions with different water fractions (Figure S5–S6). Additionally, three of the molecules (TCPP, Ce6 and NCBS) are commercially available photosensitizers. Semiconducting polymer (PF-MEHPPV) was used as the afterglow substrate to be encapsulated in the amphiphilic triblock copolymer (PEG-*b*-PPG-*b*-PEG) to form the SPN-PF-MEHPPV by nanoprecipitation (Figure 1b). In this way, WDH-001, WDH-006, TPAM-2, TCPP, Ce6 and NCBS were doped with PF-MEHPPV and encapsulated with PEG-*b*-PPG-*b*-PEG to prepare SPN-001, SPN-006, SPN-TPAM-2, SPN-TCPP, SPN-Ce6, and SPN-PF-NCBS, respectively.

The morphology and diameter of the as-prepared SPNs were characterized by transmission electron microscopy and dynamic light scattering analysis. The SPNs displayed spherical nanoparticles (Figure S7–S13) with the hydrodynamic diameters of 25–35 nm (Figure 1c). Meanwhile, these SPNs exhibited good stability in aqueous solution at least for a month (Figure S14–S20).

The optical properties of the as-prepared SPNs were further characterized by fluorescence and UV-vis absorption spectroscopy. The fluorescence spectra of SPNs were measured in the range of 500 to 800 nm (Figure 1d). SPN-PF-MEHPPV showed broad fluorescence spectra in the range of 500–700 nm. SPN-001, SPN-006, SPN-TPAM-2 gave the maximum emission at 590, 550 and 621 nm, respectively. SPN-Ce6, SPN-PF-NCBS and SPN-TCPP exhibited several fluorescence peaks, one in 500–550 nm and the others in near-infrared (NIR) region (681, 787, 655 and 725 nm, respectively). The fluorescence spectra of SPNs after doping with six photosensitizers were distinct, primarily due to the energy transfer between the PF-MEHPPV and the photosensitizer molecules (Figure S21).[14] SPNs after doping showed broad absorption bands in the range of 200–520 nm (Figure S22 and S23). Moreover, SPN-TCPP, SPN-Ce6 and SPN-PF-NCBS also showed absorption peaks at NIR region, depending on the doped TCPP, Ce6, and NCBS molecules (Figure S24, S25). Thus,

SPN-TCPP, SPN-Ce6 and SPN-PF-NCBS were irradiated by red LED (650 ± 10 nm) light while SPN-001, SPN-006 and SPN-TPAM-2 were irradiated by white LED light in the following studies. The emission spectrum of the used white LED light is shown in Figure S26.

Afterglow Properties of SPNs

We first compared the afterglow performance of SPN-PF-MEHPPV, SPN-001, SPN-006 and SPN-TPAM-2 after a 2-min white LED pre-irradiation to reveal the effect of the substituent group in photosensitizers. SPN-PF-MEHPPV gave the afterglow time of 5 h and the afterglow intensity of 2.24×10^6 p/sec/cm^2/sr at 15 s. SPN-001 and SPN-006 showed a similar afterglow time of *ca.* 5 h, but a slight decrease of the initial afterglow intensity (1.51×10^6, 1.42×10^6 p/sec/cm^2/sr at 15 s, respectively) (Figure 2a–2d). In contrast, SPN-TPAM-2 showed poor afterglow performance with an afterglow duration time of 1 h and an initial intensity of 6.77×10^5 p/sec/cm^2/sr. The results indicate that TPAM-2 doping had an adverse effect on the afterglow of SPNs while WDH-001 and WDH-006 doping showed little influence. This phenomenon was directly related to the electron-withdrawing effect. TPAM-2, containing six cyano groups, exhibited the strongest electron-withdrawing effect, while WDH-001, having only two cyano groups, displayed the weakest electron-withdrawing effect. Meanwhile, WDH-006, containing two additional carbonyl groups besides two cyano groups, resulted in a slightly stronger electron-withdrawing effect than WDH-001.

We then compared the afterglow performance of SPN-PF-MEHPPV, SPN-TCPP, SPN-Ce6 and SPN-PF-NCBS after a 2-min red LED pre-irradiation. SPN-PF-MEHPPV showed an afterglow time of 30 min and the afterglow intensity of 2.67×10^5 p/sec/cm^2/sr at 15 s (Figure 2e and 2f). In contrast, SPN-TCPP, SPN-Ce6, SPN-PF-NCBS exhibited much longer afterglow time (> 12 h) and stronger afterglow intensity (> 3.20×10^7 p/sec/cm^2/sr) at 15 s. In particular, SPN-Ce6 showed the longest afterglow time of 48 h while SPN-TCPP and SPN-PF-NCBS gave the afterglow time of 12 and 24 h, respectively. Meanwhile, SPN-PF-NCBS emitted the strongest afterglow intensity at 15 s (7.32×10^7 p/sec/cm^2/sr) compared with SPN-TCPP (4.19×10^7 p/sec/cm^2/sr) and SPN-Ce6 (3.20×10^7 p/sec/cm^2/sr) (Figure 2g, 2 h). The above results show that the doping of TCPP, Ce6, and NCBS significantly enhanced the afterglow performance of SPN-PF-MEHPPV under red LED light pre-illumination. NCBS doping promoted the initial luminescence intensity most significantly while Ce6 doping prolonged the afterglow time most effectively. TCPP contains four weak electron-withdrawing carboxyl groups, while Ce6 has three weak electron-withdrawing carboxyl groups. In contrast, NCBS does not have any electron-withdrawing groups. The presence of a larger number of electron-withdrawing groups in TCPP was less favorable for the enhancement of the afterglow performance of SPNs.

The effect of the doping proportion of two photosensitizers (TPAM-2 and NCBS) on the afterglow of SPNs was also investigated (Figure S27). The afterglow intensity of the SPNs decreased as the doping proportion of TPAM-2 increased. In general, NCBS doping obviously enhanced the afterglow intensity of the SPNs. Specifically, the afterglow intensity of the SPNs increased as the doping proportion of NCBS increased to 5.0 % (w/w), then decreased with further increase of the doping proportion of NCBS.

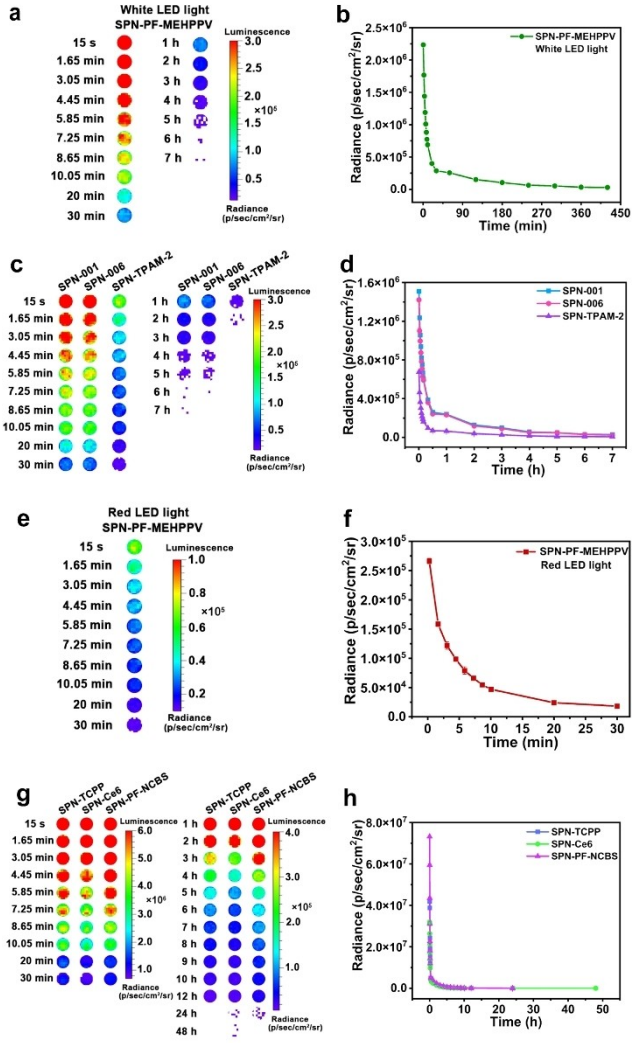

Figure 2. Afterglow decay images of SPNs at different time points and changes of radiance intensity recorded from afterglow decay images as a function of time. (a) Afterglow decay images of SPN-PF-MEHPPV after 2-min white LED illumination (0.2 W cm^{-2}). (b) Change of afterglow intensity recorded from (a). (c) Afterglow decay images of SPN-001, SPN-006 and SPN-TPAM-2 after 2-min white LED illumination (0.2 W cm^{-2}). (d) Change of afterglow intensity recorded from (c). (e) Afterglow decay images of SPN-PF-MEHPPV after 2-min red LED illumination (650 ± 10 nm, 0.07 W cm^{-2}). (f) Change of afterglow intensity recorded from (e). (g) Afterglow decay images of SPN-TCPP, SPN-Ce6 and SPN-PF-NCBS after 2-min red LED illumination (650 ± 10 nm, 0.07 W cm^{-2}). (h) Change of afterglow intensity recorded from (g). The error bars, ± one standard deviation (n = 3).

$^1O_2$ Generation Ability of SPNs

To investigate the relationship between the afterglow and the $^1O_2$ production, the $^1O_2$ generation ability of SPNs using 9,10-

anthracenediyl-bis(methylene) dimalonic acid (ABDA) as an indicator was studied. Because redox reaction along with the generation of $^1O_2$ resulted in the absorbance reduction of ABDA, the absorbance of ABDA solution in the presence of SPN-001, SPN-006 and SPN-TPAM-2, respectively, was measured after white LED light for 5 min. As shown in Figure 3a–b, SPN-TPAM-2 led to a much more significant reduction of the absorbance of ABDA than SPN-001 and SPN-006, indicating the strongest ability of SPN-TPAM-2 to produce $^1O_2$. Similarly, the absorbance of ABDA solution in the presence of SPN-TCPP, SPN-Ce6 and SPN-PF-NCBS, respectively, was measured after red LED light for 5 min to study their $^1O_2$ generation ability (Figure 3c–d). SPN-TCPP, SPN-Ce6 and SPN-PF-NCBS led to the reduction of the absorbance of ABDA to a different extent, indicating that these three SPNs had different $^1O_2$ generation abilities and SPN-Ce6 showed the strongest $^1O_2$ generation ability.

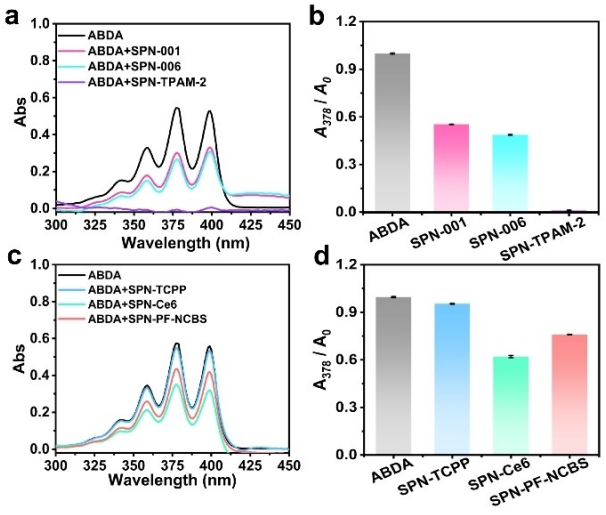

Figure 3. UV-vis absorption spectra and absorption peak ratio of ABDA in the absence and presence of different SPNs (20 μg mL^{-1}) after a pre-irradiation for 5 min. (a) ABDA in the absence and presence of SPN-001, SPN-006 and SPN-TPAM-2 after white LED pre-irradiation (0.2 W cm^{-2}). (b) UV-vis absorption peak ratio of ABDA at 378 nm (A_{378}, in the presence of SPN-001, SPN-006 and SPN-TPAM-2; A_0, in the absence of SPNs) after white LED light pre-irradiation. (c) ABDA in the absence and presence of SPN-TCPP, SPN-Ce6 and SPN-PF-NCBS after red LED irradiation(650 ± 10 nm, 0.07 W cm^{-2}). (d). UV-vis absorption peak ratio of ABDA at 378 nm after red LED light pre-irradiation. The error bars, ± one standard deviation (n = 3).

Initial Exploration of the Effect of Photosensitizers

From above results, it can be seen that for the doped photosensitizers (WDH-001, WDH-006, and TPAM-2) with strong electron-withdrawing groups, the stronger the electron-withdrawing ability of the group, the worse of the afterglow performance of the SPNs regardless of the $^1O_2$ generation ability of the photosensitizer. However, after red LED irradiation, the incorporation of TCPP, Ce6, and NCBS bearing weak or none electron-withdrawing groups significantly improved the afterglow performance of PF-MEHPPV and the $^1O_2$ generation ability played a dominant role.

To further study the impact of different light irradiation on the SPNs, UV-vis absorption of SPNs after white and red light irradiation was investigated. SPN-PF-MEHPPV appeared decreasing absorption and a lighter color under white LED illumination (Figure 4a), suggesting the molecular structure of PF-MEHPPV underwent certain change, possibly including chemical reactions and physical changes. However, under red LED light illumination, the absorption of SPN-PF-MEHPPV remained unchanged and the solution color also remained the same (Figure 4e), implying that the wavelengths within this range were not sufficient to trigger these destructive processes, thus maintaining the stability of its molecular structure.

When different molecules were doped into SPN-PF-MEHPPV, the effects on SPN-PF-MEHPPV varied significantly. Under white

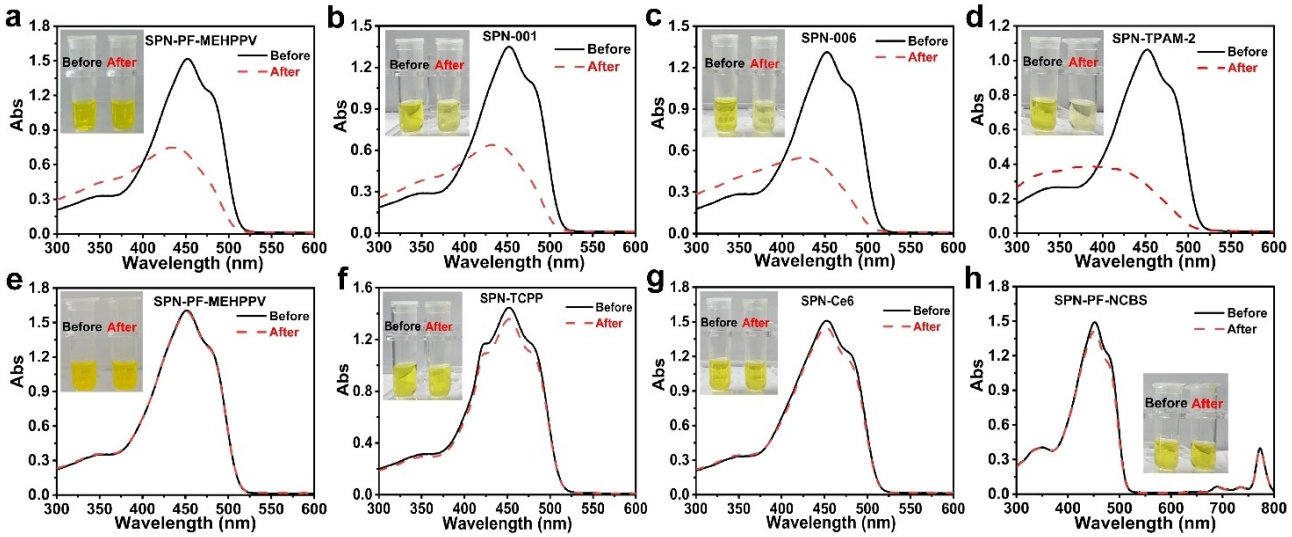

Figure 4. UV-vis absorption spectra of different SPNs (20 μg mL^{-1}) in aqueous solution before and after light pre-irradiation for 2 min. (a–d) SPN-PF-MEHPPV, SPN-001, SPN-006, and SPN-TPAM-2 after white LED pre-irradiation (0.2 W cm^{-2}). (e–h) SPN-PF-MEHPPV, SPN-TCPP, SPN-Ce6, and SPN-PF-NCBS after red LED irradiation(650 ± 10 nm, 0.07 W cm^{-2}).

light illumination, SPN-001 and SPN-006, as well as SPN-TPAM-2, exhibited a greater extent of absorption decrease. SPN-TPAM-2 showed the most significant reduction in absorbance, and the lightest color among the studied SPNs (Figure 4b–d). Moreover, SPN-TPAM-2 caused a blue shift of the absorption spectra of the SPN (Figure 4d), indicating the increase of the bond saturation in SPNs. On the contrary, under red light illumination, the absorption of SPN-TCPP, SPN-Ce6 and SPN-PF-NCBS decreased only marginally, with insignificant change in the solution color (Figure 4f–h). These results indicate that the absorption decrease in SPNs was influenced not only by the different wavelengths of light exposure but also by the presence of doping molecules.

FTIR spectroscopy was further used to investigate whether new groups were generated in PF-MEHPPV in the presence of different photosensitizers. A characteristic peak at 1739 cm^{-1} associated with C=O stretching vibrations appeared in the spectrum of pure PF-MEHPPV after white LED irradiation (Figure 5a), indicating the oxidation of vinylene bond into final carboxyl groups. In the presence of WDH-001, WDH-006 and TPAM-2, after the mixture was subjected to white light exposure, the infrared spectra not only showed a characteristic peak at 1739 (1729) cm^{-1} owing to the formation of C=O group but also exhibited characteristic peaks at 760, 818, and 1357 cm^{-1} (Figure 5b–d). These three additional peaks represented the emergence of a ternary epoxy group, corresponding to C–H out-of-plane bending vibration (760 cm^{-1}), symmetric C–O–C stretching vibration (818 cm^{-1}) and asymmetric C–O–C stretching vibration (1357 cm^{-1}), respectively.[24,25] However, no new peaks appeared and only slight change in the intensity of a few original peaks in the FTIR spectra of these pure photosensitizers, indicating the generation of new groups occurs on the PF-MEHPPV (Figure S28–30). The results indicated that the presence of TPAM-2 led to the strongest infrared characteristic peak intensities assigned to the ternary epoxy group. It has the highest efficiency in converting C=C bond of PF-MEHPPV into ternary epoxy group under white LED light illumination. The production of stable ternary epoxy group after doping with TPAM-2 in the SPNs does not involve the emission of photons, resulting in poorer afterglow performance. For comparison, the influence on the PF-MEHPPV from other three photosensitizers (TCPP, Ce6 and NCBS) were also characterized by FTIR after red LED irradiation. The spectra showed that only one main new peak at 1736 (1738/1735) cm^{-1} appeared in the absence and presence of photosensitizers after illumination (Figure 5e–5 f), indicating only the appearance of carboxyl groups. These results show that not only the dioxetane intermediate reaction, but also other reactions for the formation of ternary epoxy group occurred in the presence of WDH-001, WDH-006 and TPAM-2 under white LED irradiation.

Proton nuclear magnetic resonance (^{1}H NMR) spectra of PF-MEHPPV in the presence of TPAM-2 after white light illumination was further analyzed to reveal the multi-step reactions. Two new peaks at 10.06 and 10.47 p.p.m. appeared after light irradiation, indicating the generation of aldehyde and carboxyl respectively (Figure 6a). Two other new peaks at 4.45 and 3.02 p.p.m. were assigned to the epoxy groups at the *ortho*- and *meta*-position relative to the methoxy group of PF-MEHPPV (Figure 6b, 6c). The broadening and splitting of peaks resulted from various chemical environments and suggested the formation of heterogeneous fragments. Based on these data, a multi-step reaction mechanism was proposed to elucidate the influence of electron-withdrawing effects on the afterglow luminescence of PF-MEHPPV. Owing to the different products from distinct bond cleavage sites, one possible case was illustrated as follows. White light irradiation of PF-MEHPPV generated $^1O_2$ to oxidize partial vinylene bonds (C=C) of polymer chains to an unstable dioxetane intermediate (Figure 6d, step i). The intermediate rapidly degraded into PF-MEHPPV-aldehyde, causing chain scission. Then, the PF-

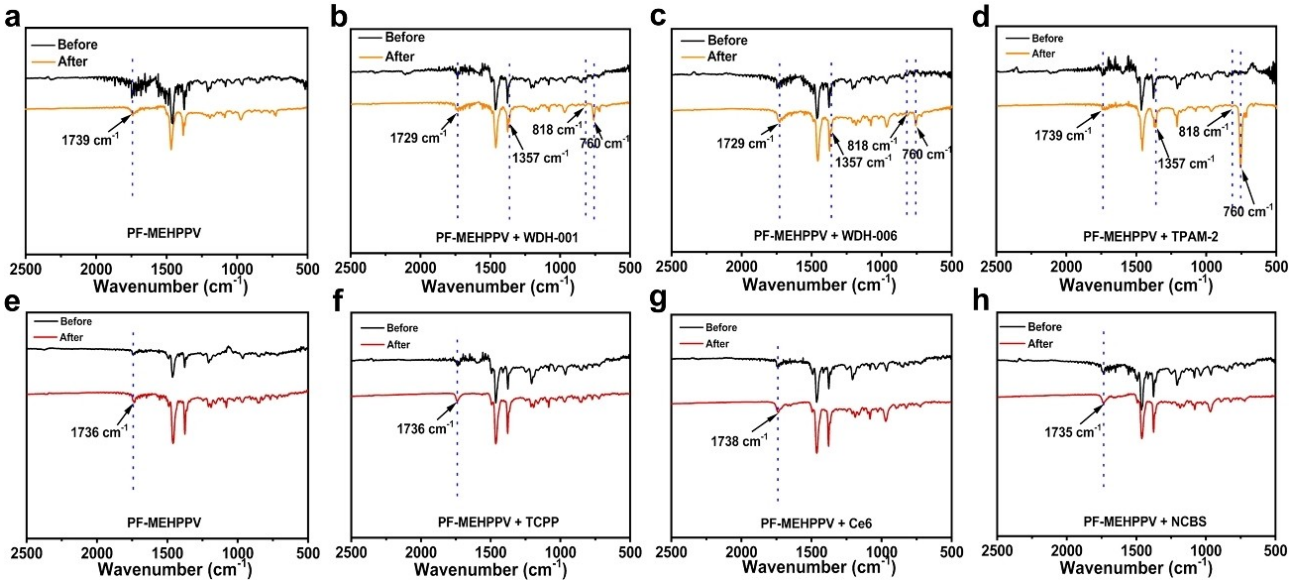

Figure 5. Effect of photosensitizer on the FT-IR spectra of PF-MEHPPV before and after light irradiation. (a–d) in the absence and presence of WDH-001, WDH-006, and TPAM-2 under white LED irradiation for 4 h, respectively. (e–h) in the absence/presence of TCPP, Ce6, and NCBS under red LED irradiation for 4 h.

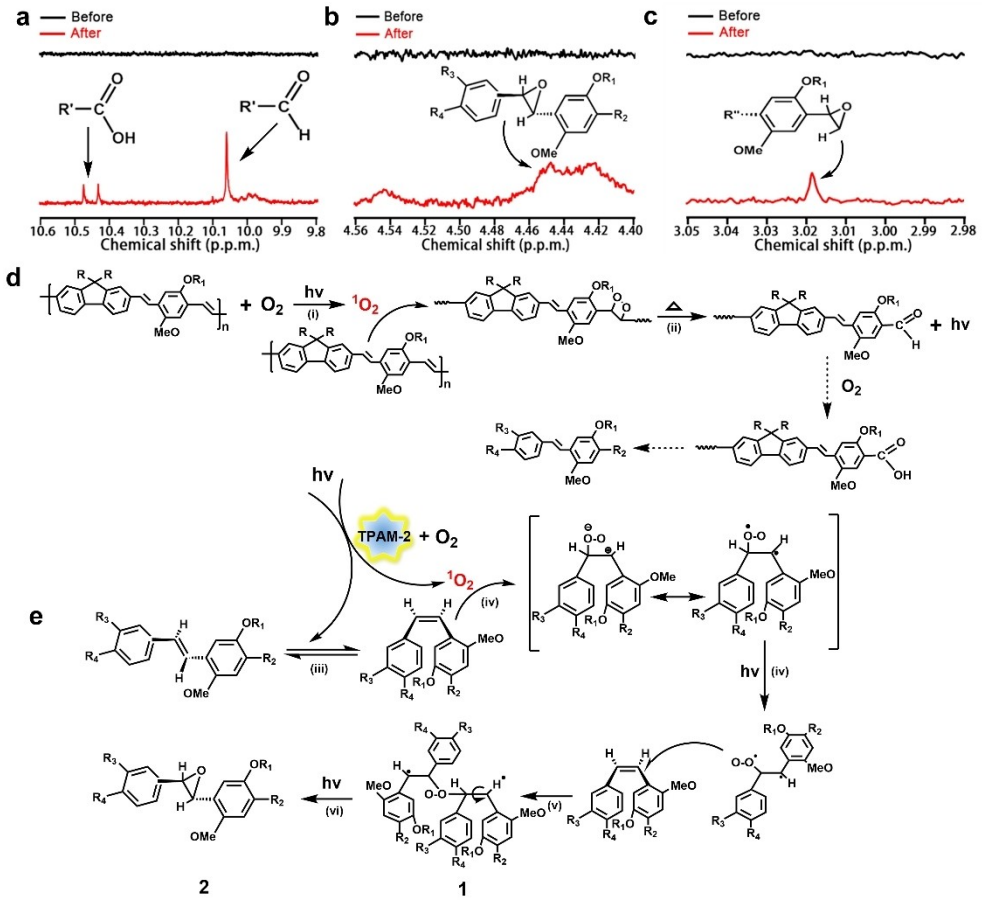

Figure 6. Mechanistic study of the afterglow of PF-MEHPPV affected by TPAM-2. (a–c) 1H NMR spectra of PF-MEHPPV in the presence of TPAM-2 before and after white light illumination (0.1 W/cm^2) for 4 h in $CDCl_3$. (d–e) Mechanistic reactions of PF-MEHPPV in the presence of TPAM-2 under white light illumination.

MEHPPV-aldehyde was further oxidized into PF-MEHPPV-carboxyl (Figure 6d, step ii). The chain scission made PF-MEHPPV exist in the form of stilbene unit with substituents, which still contained a vinylene moiety. These stilbene units underwent photoisomerization, resulting in the transformation between *cis-trans* isomers under light exposure (Figure 6d, step iii).[25] While in the presence of TPAM-2, light irradiation of TPAM-2 generated highly reactive $^1O_2$ that reacted with vinylene bond (C=C) of stilbene. When the electron deficient $^1O_2$ interacted with relatively electron rich π bond in stilbene and subject to strong electron-withdrawing influence, one oxygen atom was initially added onto the double bond to create a transient intermediate due to large delocalization on the π systems (Figure 6e, step iv).[26] Then, this intermediate reacted with another *cis*-stilbene, forming product 1 and final transferring into product 2 with ternary epoxy group (Figure 6e, step v–vi). This process did not involve the emission of photons, leading to poor afterglow performance of the SPNs.

Conclusions

In summary, we have reported the afterglow performance of phenylenevinylene-based semiconducting polymer nanoparticles doped with photosensitizers containing electron-withdrawing groups. Six photosensitizers with different electron-drawing substituents were doped into SPNs and irradiated under white and red LED light, respectively. The afterglow performance of SPNs was significantly influenced by doping with photosensitizers bearing electron-withdrawing groups. For the doped photosensitizers WDH-001, WDH-006, and TPAM-2 bearing strong electron-withdrawing groups, the stronger the electron-withdrawing ability of the group, the worse of the afterglow performance of the SPN regardless of the $^1O_2$ generation ability of the photosensitizer. For the doped photosensitizers such as TCPP, Ce6 and NCBS bearing weak or none electron-withdrawing groups, the $^1O_2$ generation ability of photosensitizer played a dominant role in the SPN's afterglow performance. Under white light illumination, WDH-001, WDH-006 and TPAM-2 cause the formation of ternary epoxy groups on the PF-MEHPPV backbone, resulting in deteriorated afterglow performance. This work is helpful in guiding the design and fabrication of SPNs with different afterglow properties.

Acknowledgements

This work was supported by the National Natural Science Foundation of China (No. 21934002), Natural Science Foundation of Jiangsu Province, China (No. BK20231491) and the Collaborative Innovation Center of Food Safety and Quality Control in Jiangsu Province.

Conflict of Interests

The authors declare no conflict of interest.

Data Availability Statement

The data that support the findings of this study are available from the corresponding author upon reasonable request.

Keywords: Semiconducting polymer nanoparticles · photosensitizer doping · electron-withdrawing group · afterglow performance

[1] C. Liu, K. Wang, X. Gong, A. J. Heeger, *Chem. Soc. Rev.* **2016**, *45*(17), 4825–4846.
[2] A. Facchetti, *Chem. Mater.* **2010**, *23*(3), 733–758.
[3] C. F. Wu, D. T. Chiu, *Angew. Chem. Int. Ed.* **2013**, *52*(11), 3086–3109.
[4] K. Li, B. Liu, *Chem. Soc. Rev.* **2014**, *43*(18), 6570–6597.
[5] C. Zhu, L. Liu, Q. Yang, F. Lv, S. Wang, *Chem. Rev.* **2012**, *112*(8), 4687–4735.
[6] P. P. Gai, W. Yu, H. Zhao, R. L. Qi, F. Li, L. B. Liu, F. T. Lv, S. Wang, *Angew. Chem. Int. Ed.* **2020**, *59*(18), 7224–7229.
[7] M. Palner, K. Y. Pu, S. Shao, J. H. Rao, *Angew. Chem. Int. Ed.* **2015**, *54*(39), 11477–11480.
[8] M. Peters, S. Seneca, N. Hellings, T. Junkers, A. Ethirajan, *Colloids Surf. B* **2018**, *169*, 494–501.
[9] D. Kim, K. Shin, S. G. Kwon, T. Hyeon, *Adv. Mater.* **2018**, *30*(49), 1802309.
[10] Y. H. Chan, P. J. Wu, *Part. Part. Syst. Charact.* **2014**, *32*(1), 11–28.
[11] H. Ou, J. LI, C. Chen, H. Q. Gao, X. Xue, D. Ding, *Sci. China Mater.* **2019**, *62*(11), 1740–1758.
[12] P. Marlow, F. Manger, K. Fischer, C. Sprau, A. Colsmann, *Nanoscale.* **2022**, *14*(14), 5569–5578.
[13] H. C. Leventis, S. P. King, A. Sudlow, M. S. Hill, K. C. Molloy, S. A. Haque, *Nano Lett.* **2010**, *10*(4), 1253–1258.
[14] C. Yin, X. Zhen, H. Zhao, Y. F. Tang, Y. Ji, Y. Lyu, Q. L. Fan, W. Huang, K. Y. Pu, *ACS Appl. Mater. Interfaces.* **2017**, *9*(14), 12332–12339.
[15] Q. Q. Miao, C. Xie, X. Zhen, Y. Lyu, H. W. Duan, X. G. Liu, J. V. Jokerst, K. Y. Pu, *Nat. Biotechnol.* **2017**, *35*(11), 1102–1110.
[16] Y. Y. Jiang, J. G. Huang, X. Zhen, Z. L. Zeng, J. C. Li, C. Xie, Q. Q. Miao, J. Chen, P. Chen, K. Y. Pu, *Nat. Commun.* **2019**, *10*(1), 2064.
[17] Y. Xu, W. T. Yang, D. F. Yao, K. X. Bian, W. W. Zeng, K. Liu, D. B. Wang, B. B. Zhang, *Chem. Sci.* **2020**, *11*(2), 419–428.
[18] X. Ni, X. Y. Zhang, X. C. Duan, H. L. Zheng, X. S. Xue, D. Ding, *Nano Lett.* **2018**, *19*(1), 318–330.
[19] Y. Lyu, D. Cui, J. G. Huang, W. X. Fan, Y. S. Miao, K. Y. Pu, *Angew. Chem. Int. Ed.* **2019**, *58*(15), 4983–4987.
[20] L. Y. Wu, Y. Ishigaki, Y. Y. Hu, K. Sugimoto, W. H. Zeng, T. Harimoto, Y. D. Sun, J. He, T. Suzuki, X. Q. Jiang, H.-Y. Chen, D. J. Ye, *Nat. Commun.* **2020**, *11*(1), 446.
[21] C. Xie, X. Zhen, Q. Q. Miao, Y. Lyu, K. Y. Pu, *Adv. Mater.* **2018**, *30*(21), 1801331.
[22] D. H. Wang, L. J. Chen, X. Zhao, X. P. Yan, *Talanta.* **2021**, *225*, 122046.
[23] R. M. Silverstein, G. C. Bassler, *J. Chem. Educ.* **1962**, *39*(11), 546.
[24] H. J. Yu, L. Wang, J. Huo, Q. H. Tan, J. M. Gao, *Des. Monomers Polym.* **2008**, *11*(4), 347–356.
[25] S. S. M. Kalajahi, M. Hajimohammadi, N. Safari, *React. Kinet. Mech. Catal.* **2014**, *113*(2), 629–640.
[26] J. B. Birks, *Chem. Phys.* Letters. **1976**, *38*(3), 437–440.

Manuscript received: March 7, 2024
Accepted manuscript online: April 24, 2024
Version of record online: June 3, 2024